

Higgs Boson Production in Association with Bottom Quarks

J. Campbell^(a), S. Dawson^(b), S. Dittmaier^(c), C. Jackson^(d), M. Krämer^(e), F. Maltoni^(f), L. Reina^(d), M. Spira^(g), D. Wackerlo^(h), S. Willenbrock⁽ⁱ⁾

(a) High Energy Physics Division, Argonne National Laboratory, Argonne, IL 60439, USA

(b) Physics Department, Brookhaven National Laboratory, Upton, N.Y. 11973, USA

(c) Max-Planck-Institut für Physik, Föhringer Ring 6, D-80805 München, Germany

(d) Physics Department, Florida State University, Tallahassee, FL 32306, USA

(e) School of Physics, The University of Edinburgh, Edinburgh EH9 3JZ, Scotland

(f) Centro Studi e Ricerche Enrico Fermi, via Panisperna 89/A, 00184 Rome, Italy

(g) Paul Scherrer Institut PSI, CH-5232 Villigen PSI, Switzerland

(h) Department of Physics, State University of New York at Buffalo, Buffalo, N.Y. 14260, USA

(i) Department of Physics, University of Illinois at Urbana-Champaign, Urbana, IL 61801, USA

Abstract

In the Standard Model, the coupling of the Higgs boson to b quarks is weak, leading to small cross sections for producing a Higgs boson in association with b quarks. However, Higgs bosons with enhanced couplings to b quarks, such as occur in supersymmetric models for large values of $\tan \beta$, will be copiously produced at both the Tevatron and the LHC in association with b quarks which will be an important discovery channel. We investigate the connections between the production channels, $bg \rightarrow bh$ and $gg \rightarrow b\bar{b}h$, at next-to-leading order (NLO) in perturbative QCD and present results for the case with two high- p_T b jets and with one high- p_T b jet at both the Tevatron and the LHC. Finally, the total cross sections without cuts are compared between $gg \rightarrow b\bar{b}h$ at NLO and $b\bar{b} \rightarrow h$ at NNLO.

1. Introduction

In the Standard Model, the production of a Higgs boson in association with b quarks is suppressed by the small size of the Yukawa coupling, $g_{bh} = m_b/v \sim 0.02$. However, in a supersymmetric theory with a large value of $\tan \beta$, the b -quark Yukawa coupling can be strongly enhanced, and Higgs production in association with b quarks becomes the dominant production mechanism.

In a four-flavor-number scheme with no b quarks in the initial state, the lowest order processes are the tree level contributions $gg \rightarrow b\bar{b}h$ and $q\bar{q} \rightarrow b\bar{b}h$, illustrated in Fig. 1. The inclusive cross section for $gg \rightarrow b\bar{b}h$ develops potentially large logarithms proportional to $L_b \equiv \log(Q^2/m_b^2)$ which arise from the splitting of gluons into $b\bar{b}$ pairs.¹ Since $Q \gg m_b$, the splitting is intrinsically of $\mathcal{O}(\alpha_s L_b)$, and because the logarithm is potentially large, the convergence of the perturbative expansion may be poor. The convergence can be improved by summing the collinear logarithms to all orders in perturbation theory through the use of b quark parton distributions (the five-flavor-number scheme) [4] at the factorization scale $\mu_F = Q$. This approach is based on the approximation that the outgoing b quarks are at small transverse momentum. Thus the incoming b partons are given zero transverse momentum at leading order, and acquire transverse momentum at higher order. In the five-flavor-number scheme, the counting of perturbation theory involves both α_s and $1/L_b$. In this scheme, the lowest order inclusive process is $b\bar{b} \rightarrow h$, see Fig. 2. The first order corrections contain the $\mathcal{O}(\alpha_s)$ corrections to $b\bar{b} \rightarrow h$ and the tree

¹It should be noted that the b mass in the argument of the logarithm arises from collinear $b\bar{b}$ configurations, while the large scale Q stems from b transverse momenta of this order, up to which factorization is valid. The scale Q is the end of the collinear region, which is expected to be of the order of $M_h/4$ [1, 2, 3].

level process $gb \rightarrow bh$, see Fig. 3, which is suppressed by $\mathcal{O}(1/L_b)$ relative to $b\bar{b} \rightarrow h$ [5]. It is the latter process which imparts transverse momentum to the b quarks. The relevant production mechanism depends on the final state being observed. For inclusive Higgs production it is $b\bar{b} \rightarrow h$, while if one demands that at least one b quark be observed at high- p_T , the leading partonic process is $gb \rightarrow bh$. Finally, if two high- p_T b quarks are required, the leading subprocess is $gg \rightarrow b\bar{b}h$.

The leading order (LO) predictions for these processes have large uncertainties due to the strong dependence on the renormalization/factorization scales and also due to the scheme dependence of the b -quark mass in the Higgs b -quark Yukawa coupling. The scale and scheme dependences are significantly reduced when higher-order QCD corrections are included.

Section 2 describes the setup for our analysis, and in Section 3 we compare the LO and NLO QCD results for the production of a Higgs boson with two high- p_T b jets. Section 4 contains a discussion of the production of a Higgs boson plus one high- p_T b jet at NLO, including a comparison of results within the four-flavor-number and the five-flavor-number schemes. We consider the corresponding inclusive Higgs cross sections in Section 5. Although motivated by the MSSM and the possibility for enhanced b quark Higgs boson couplings, all results presented here are for the Standard Model. To a very good approximation the corresponding MSSM results can be obtained by rescaling the bottom Yukawa coupling [6, 7].



Fig. 1: Sample Feynman diagrams for $gg \rightarrow b\bar{b}h$ and $q\bar{q} \rightarrow b\bar{b}h$ production.

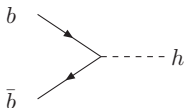


Fig. 2: Feynman diagram for $b\bar{b} \rightarrow h$ production.



Fig. 3: Feynman diagrams for $gb \rightarrow bh$ production.

2. Setup

All results are obtained using the CTEQ6L1 parton distribution functions (PDFs) [8] for lowest order cross sections and CTEQ6M PDFs for NLO results. The top quark is decoupled from the running of $m_b(\mu)$ and $\alpha_s(\mu)$ and the NLO (LO) cross sections are evaluated using the 2 (1)-loop evolution of $\alpha_s(\mu)$ with $\alpha_s^{NLO}(M_Z) = 0.118$. We use the $\overline{\text{MS}}$ running b quark mass, $m_b(\mu)$, evaluated at 2 (1)-loop for σ_{NLO} (σ_{LO}), with the b pole mass taken as $m_b = 4.62$ GeV. The dependence of the rates on the renormalization (μ_R) and factorization (μ_F) scales is investigated [5, 6, 7, 9, 10] in order to estimate the uncertainty of the predictions for the inclusive Higgs production channel and for the Higgs plus 1 b -jet channel. The dependence of the Higgs plus 2 b -jet rates on the renormalization (μ_R) and factorization

(μ_F) scales has been investigated elsewhere [6, 7] and here we fix $\mu = \mu_R = \mu_F = (2m_b + M_h)/4$, motivated by the studies in Refs. [1, 2, 3, 5, 6, 7, 9, 10].

In order to reproduce the experimental cuts as closely as possible for the case of Higgs plus 1 or 2 high- p_T b quarks, we require the final state b and \bar{b} to have a pseudorapidity $|\eta| < 2$ for the Tevatron and $|\eta| < 2.5$ for the LHC. To better simulate the detector response, the gluon and the b/\bar{b} quarks are treated as distinct particles only if the separation in the azimuthal angle-pseudorapidity plane is $\Delta R > 0.4$. For smaller values of ΔR , the four-momentum vectors of the two particles are combined into an effective $b\bar{b}$ quark momentum four-vector. All results presented in the four-flavor-number scheme have been obtained independently by two groups with good agreement [6, 7, 11, 12].

3. Higgs + 2 b Jet Production

Requiring two high- p_T bottom quarks in the final state reduces the signal cross section with respect to that of the zero and one b -tag cases, but it also greatly reduces the background. It also ensures that the detected Higgs boson has been radiated off a b or \bar{b} quark and the corresponding cross section is therefore unambiguously proportional to the square of the b -quark Yukawa coupling at leading order, while at next-to-leading order this property is mildly violated by closed top-quark loops [6, 7]. The parton level processes relevant at lowest order are $gg \rightarrow b\bar{b}h$ and $q\bar{q} \rightarrow b\bar{b}h$, as illustrated in Fig. 1. Searches for the neutral MSSM Higgs bosons h, H, A produced in association with b quarks have been performed at the Tevatron [13].

The rate for Higgs plus 2 high- p_T b jets has been computed at NLO QCD in Refs. [6, 7] and is shown in Fig. 4 for both the Tevatron and the LHC. The NLO QCD corrections modify the LO predictions by $\lesssim 30\%$ at the Tevatron and $\lesssim 50\%$ at the LHC. The total cross section plots include a cut on $p_T^{b/\bar{b}} > 20$ GeV, which has a significant effect on the cross sections. We show the dependence of the cross section on this cut in Fig. 5. The NLO corrections are negative at large values of the cut on $p_T^{b/\bar{b}}$ and tend to be positive at small values of $p_T^{b/\bar{b}}$.

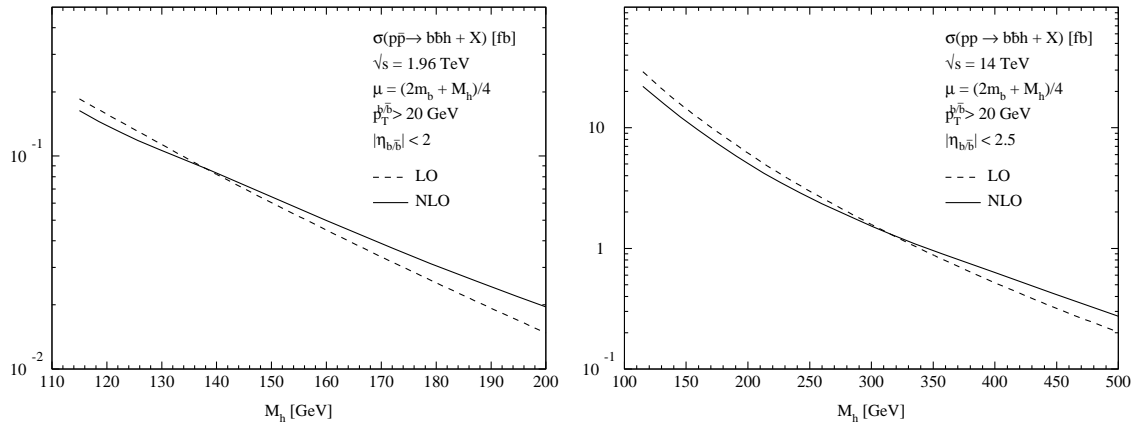


Fig. 4: Total cross sections for $p\bar{p}(pp) \rightarrow b\bar{b}h + X$ at the Tevatron and the LHC as a function of the Higgs mass M_h with two high- p_T b jets identified in the final state. The b/\bar{b} quarks are required to satisfy $p_T^{b/\bar{b}} > 20$ GeV. We fix $\mu = \mu_R = \mu_F = (2m_b + M_h)/4$.

4. Higgs + 1 b Jet Production

The associated production of a Higgs boson plus a single b quark (or \bar{b} quark) is a promising channel for Higgs production in models with enhanced $b\bar{b}h$ couplings. The cross section is an order of magnitude larger than that for Higgs plus 2 high- p_T b jet production for the cuts imposed in our analysis.

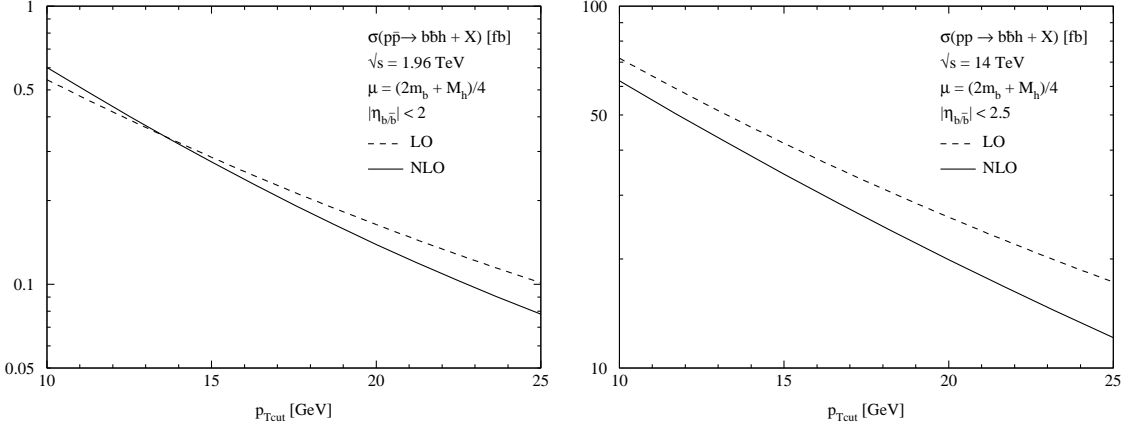


Fig. 5: Total cross sections for $p\bar{p}(pp) \rightarrow b\bar{b}h + X$ at the Tevatron and the LHC as a function of the cut $p_{T\text{cut}}$ in $p_T^{b,\bar{b}}$ for a Higgs mass $M_h = 120$ GeV with two high- p_T b jets identified in the final state. We fix $\mu = \mu_R = \mu_F = (2m_b + M_h)/4$.

In the four-flavor-number scheme, this process has been computed to NLO, with the momentum of one of the b quarks integrated over [6, 11, 12]. This integration yields a potentially large factor L_b . Both the total cross sections and the dependence on the $p_T^{b,\bar{b}}$ cut at the Tevatron and the LHC are shown in Figs. 6 and 7. The NLO corrections increase the cross section by $\lesssim 50\%$ at the Tevatron and $\lesssim 80\%$ at the LHC. The renormalization/factorization scales are varied around the central value $\mu = \mu_R = \mu_F \equiv (2m_b + M_h)/4$. At the Tevatron, the upper bands of the curves for the four-flavor-number scheme in Figs. 6 and 7 correspond to $\mu_R = \mu_F = 2\mu$, while the lower bands correspond to $\mu_R = \mu_F = \mu/2$. The scale dependence is more interesting at the LHC, where the upper bands are obtained with $\mu_R = \mu/2$ and $\mu_F = 2\mu$, while the lower bands correspond to $\mu_R = 2\mu$ and $\mu_F = \mu/2$. At both the Tevatron and the LHC, the width of the error band below the central value ($\mu = \mu_R = \mu_F$) is larger than above.

In the five-flavor-number scheme, the NLO result consists of the lowest order process, $bg \rightarrow bh$, along with the $\mathcal{O}(\alpha_s)$ and $\mathcal{O}(1/L_b)$ corrections, which are of moderate size for our scale choices [9]. The potentially large logarithms L_b arising in the four-flavor-number scheme have been summed to all orders in perturbation theory by the use of b quark PDFs. In the five-flavor-number scheme, the upper bands of the curves for the Tevatron in Figs. 6 and 7 correspond to $\mu_R = \mu$ and $\mu_F = 2\mu$, while the lower bands correspond to $\mu_R = \mu/2$ and $\mu_F = \mu$. At the LHC, the upper bands are obtained with $\mu_R = \mu$ and $\mu_F = 2\mu$, while the lower bands correspond to $\mu_R = 2\mu$ and $\mu_F = \mu/2$. The two approaches agree within their scale uncertainties, but the five-flavor-number scheme tends to yield larger cross sections as can be inferred from Figs. 6 and 7.

Contributions involving closed top-quark loops have not been included in the five-flavor-number scheme calculation of Ref. [9]. This contribution is negligible in the MSSM for large $\tan\beta$. In the four-flavor scheme, the closed top-quark loops have been included and in the Standard Model reduce the total cross section for the production of a Higgs boson plus a single b jet by $\sim -7\%$ at the Tevatron and $\sim -13\%$ at the LHC for $M_h = 120$ GeV [11, 12].

5. Inclusive Higgs Boson Production

If the outgoing b quarks are not observed, then the dominant process for Higgs production in the five-flavor-number scheme at large values of $\tan\beta$ is $b\bar{b} \rightarrow h$. This final state contains two spectator b quarks (from the gluon splittings) which tend to be at low transverse momentum. At the LHC this state can be identified through the decays into $\mu^+\mu^-$ and $\tau^+\tau^-$ for the heavy Higgs bosons H, A at large values of $\tan\beta$ in the MSSM [14]. The $b\bar{b} \rightarrow h$ process has been computed to NLO [5] and NNLO [10] in perturbative QCD. The rate depends on the choice of renormalization/factorization scale $\mu_{R/F}$, and at

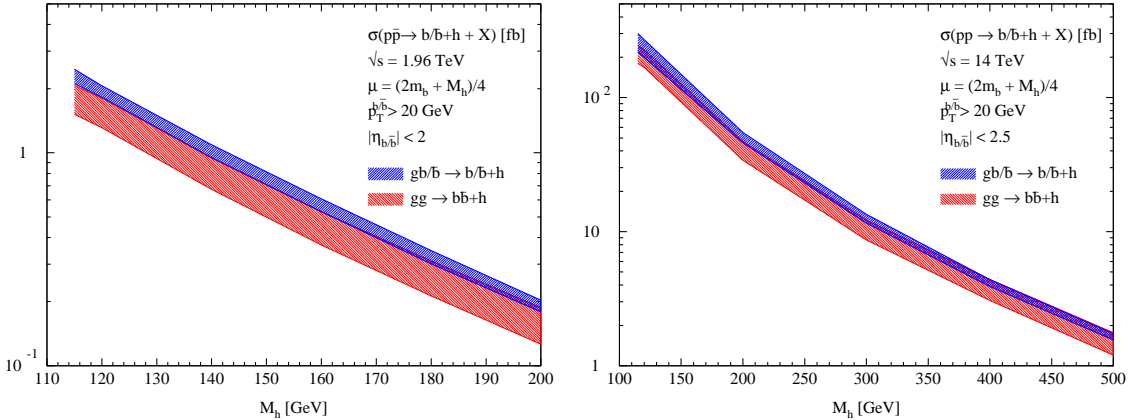


Fig. 6: Total cross sections for $p\bar{p}(pp) \rightarrow b\bar{b}h + X$ at the Tevatron and the LHC as a function of the Higgs mass M_h with one high- p_T b jet identified in the final state. The $b(\bar{b})$ quark is required to satisfy $p_T^{b/\bar{b}} > 20$ GeV. We vary the renormalization/factorization scales around the central value $\mu = \mu_R = \mu_F = (2m_b + M_h)/4$ as described in the text.

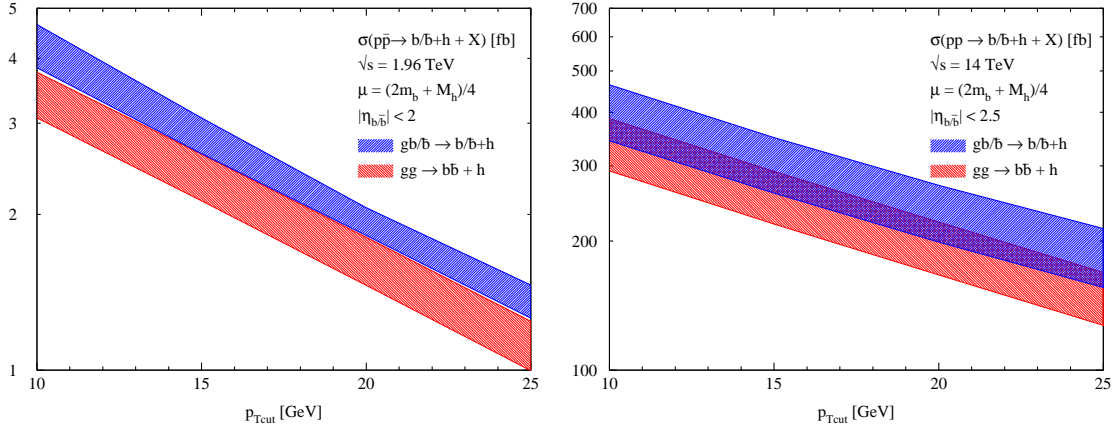


Fig. 7: Total cross sections for $p\bar{p}(pp) \rightarrow b\bar{b}h + X$ at the Tevatron and the LHC as a function of the cut $p_{T\text{cut}}$ in $p_T^{b/\bar{b}}$ for a Higgs mass $M_h = 120$ GeV with one high- p_T b jet identified in the final state. We vary the renormalization/factorization scales around the central value $\mu = \mu_R = \mu_F = (2m_b + M_h)/4$ as described in the text.

NLO a significant scale dependence remains. The scale dependence becomes insignificant at NNLO. It has been argued that the appropriate factorization scale choice is $\mu_F = (M_h + 2m_b)/4$ [2, 3] and it is interesting to note that at this scale, the NLO and NNLO results nearly coincide [10].

An alternative calculation is based on the processes $gg \rightarrow b\bar{b}h$ and $q\bar{q} \rightarrow b\bar{b}h$ (four-flavor-number scheme), which has been calculated at NLO [6, 11, 12]. Despite the presence of the logarithms L_b in the calculation based on $gg \rightarrow b\bar{b}h$, which are not resummed, it yields a reliable inclusive cross section, as evidenced by Fig. 8. A sizeable uncertainty due to the renormalization and factorization scale dependence remains which might reflect that the logarithms L_b are not resummed in this approach, so that the perturbative convergence is worse than in the corresponding case of $t\bar{t}h$ production [15]. In the Standard Model, the closed top-quark loops have been included in the four-flavor-number calculation and reduce the inclusive NLO total cross section for $pp(p\bar{p}) \rightarrow b\bar{b}h$ by $\sim -4\%$ at the Tevatron and $\sim -9\%$ at the LHC for $M_h = 120$ GeV [11, 12]. In the MSSM, the closed top quark loops are negligible for large $\tan\beta$ [6, 7].

The NLO four-flavor-number scheme calculation is compared with the NNLO calculation of $b\bar{b} \rightarrow h$ (five-flavor-number scheme) in Fig. 8. The two calculations agree within their respective scale uncertainties for small Higgs masses, while for large Higgs masses the five-flavor-number scheme tends

to yield larger cross sections. Note that closed top-quark loops have not been included in the NNLO calculation of $b\bar{b} \rightarrow h$ [10].

To all orders in perturbation theory the four- and five-flavor number schemes are identical, but the way of ordering the perturbative expansion is different and the results do not match exactly at finite order. The quality of the approximations in the two calculational schemes is difficult to quantify, and the residual uncertainty of the predictions may not be fully reflected by the scale variation displayed in Fig. 8.

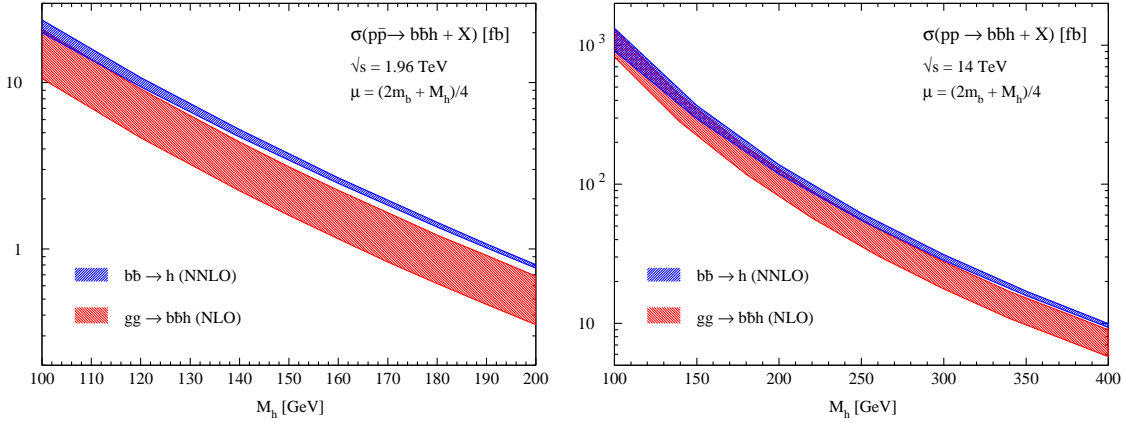


Fig. 8: Total cross sections for $p\bar{p}(pp) \rightarrow b\bar{b}h + X$ at the Tevatron and the LHC as a function of the Higgs mass M_h with no b jet identified in the final state. The error bands correspond to varying the scale from $\mu_R = \mu_F = (2m_b + M_h)/8$ to $\mu_R = \mu_F = (2m_b + M_h)/2$. The NNLO curves are from Ref. [10].

6. Conclusions

We investigated $b\bar{b}h$ production at the Tevatron and the LHC, which is an important discovery channel for Higgs bosons at large values of $\tan\beta$ in the MSSM, where the bottom Yukawa coupling is strongly enhanced [13, 14]. Results for the cross sections with two tagged b jets have been presented at NLO including transverse-momentum and pseudorapidity cuts on the b jets which are close to the experimental requirements. The NLO corrections modify the predictions by up to 50% and reduce the theoretical uncertainties significantly. For the cases of one and no tagged b jet in the final state we compared the results in the four- and five-flavor-number schemes. Due to the smallness of the b quark mass, large logarithms L_b might arise from phase space integration in the four-flavor-number scheme, which are resummed in the five-flavor-number scheme by the introduction of evolved b parton densities. The five-flavor-number scheme is based on the approximation that the outgoing b quarks are at small transverse momentum. Thus the incoming b partons are given zero transverse momentum at leading order, and acquire transverse momentum at higher order. The two calculational schemes represent different perturbative expansions of the same physical process, and therefore should agree at sufficiently high order. It is satisfying that the NLO (and NNLO) calculations presented here agree within their uncertainties. This is a major advance over several years ago, when comparisons of $b\bar{b} \rightarrow h$ at NLO and $gg \rightarrow b\bar{b}h$ at LO were hardly encouraging [1, 16].

7. Acknowledgement

We thank the organizers of the 2003 Les Houches workshop for organizing such a productive and interesting workshop.

References

- [1] D. Rainwater, M. Spira and D. Zeppenfeld, Proceedings “Physics at TeV Colliders”, Les Houches, France, 2001, hep-ph/0203187;
M. Spira, Proceedings “SUSY02”, Hamburg, Germany, 2002, hep-ph/0211145.
- [2] F. Maltoni, Z. Sullivan and S. Willenbrock, *Phys. Rev.* **D67** (2003) 093005.
- [3] E. Boos and T. Plehn, *Phys. Rev.* **D69** (2004) 094005;
T. Plehn, *Phys. Rev.* **D67** (2003) 014018.
- [4] R.M. Barnett, H.E. Haber and D.E. Soper, *Nucl. Phys.* **B306** (1988) 697;
F. I. Olness and W.-K. Tung, *Nucl. Phys.* **B308** (1988) 813;
D. Dicus and S. Willenbrock, *Phys. Rev.* **D39** (1989) 751.
- [5] D. Dicus, T. Stelzer, Z. Sullivan and S. Willenbrock, *Phys. Rev.* **D59** (1999) 094016;
C. Balazs, H.-J. He and C.P. Yuan, *Phys. Rev.* **D60** (1999) 114001.
- [6] S. Dittmaier, M. Krämer and M. Spira, hep-ph/0309204.
- [7] S. Dawson, C. Jackson, L. Reina and D. Wackerth, *Phys. Rev.* **D69** (2004) 074027.
- [8] J. Pumplin *et. al.*, *JHEP* **0207** (2002) 012; D. Stump *et. al.*, *JHEP* **0310** (2003) 046.
- [9] J. Campbell, R. K. Ellis, F. Maltoni and S. Willenbrock, *Phys. Rev.* **D67** (2003) 095002.
- [10] R. Harlander and W. Kilgore, *Phys. Rev.* **D68** (2003) 013001.
- [11] S. Dittmaier, M. Krämer and M. Spira, paper in preparation.
- [12] S. Dawson, C. Jackson, L. Reina and D. Wackerth, paper in preparation.
- [13] T. Affolder *et al.* [CDF Collaboration], *Phys. Rev. Lett.* **86** (2001) 4472.
- [14] ATLAS Collaboration, Technical Design Report, CERN–LHCC 99–14 (May 1999);
CMS Collaboration, Technical Proposal, CERN–LHCC 94–38 (December 1994);
S. Dawson, D. Dicus, C. Kao, and R. Malhotra, hep-ph/0402172.
- [15] W. Beenakker, S. Dittmaier, M. Krämer, B. Plümper, M. Spira and P.M. Zerwas, *Phys. Rev. Lett.* **87** (2001) 201805, *Nucl. Phys.* **B653** (2003) 151;
L. Reina and S. Dawson, *Phys. Rev. Lett.* **87** (2001) 201804;
L. Reina, S. Dawson and D. Wackerth, *Phys. Rev.* **D65** (2002) 053017;
S. Dawson, L.H. Orr, L. Reina and D. Wackerth, *Phys. Rev.* **D67** (2003) 071503;
S. Dawson, C. Jackson, L.H. Orr, L. Reina and D. Wackerth, *Phys. Rev.* **D68** (2003) 034022.
- [16] M. Carena *et al.*, Report of the Tevatron Higgs Working Group, hep-ph/0010338.